Supporting Information

CDs "inserted" abundant FeB based electrode *via* "local photothermal effect" strategy toward efficient overall seawater splitting

Shiheng Liang[a], Liugang Wu[a], Yiming Wang[a], Yuqi Shao[a], Hongyuan Song[c], Ziliang Chen[b], Weiju Hao*[a]

[a]School of Materials and Chemistry, University of Shanghai for Science and Technology, Shanghai 200093, P. R. China

[b]Institute of Functional Nano and Soft Materials (FUNSOM), Jiangsu Key Laboratory for Carbon-based Functional Materials and Devices, Joint International Research Laboratory of Carbon-Based Functional Materials and Devices, Soochow University, Suzhou 215123, Jiangsu, China

[c]Department of Ophthalmology, Shanghai Changhai Hospital, Shanghai, 200433, P.R. China

E-mail: wjhao@usst.edu.cn

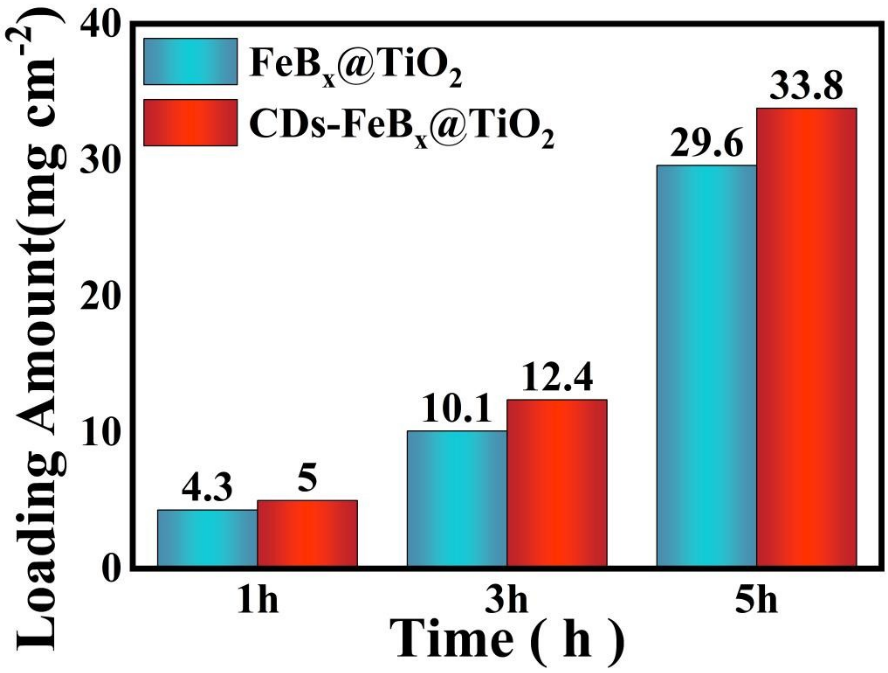

Figure S1. $FeB_x@TiO_2$ and CDs-$FeB_x@TiO_2$ electrodes are electroless plated for 1h, 3h, and 5h, respectively.

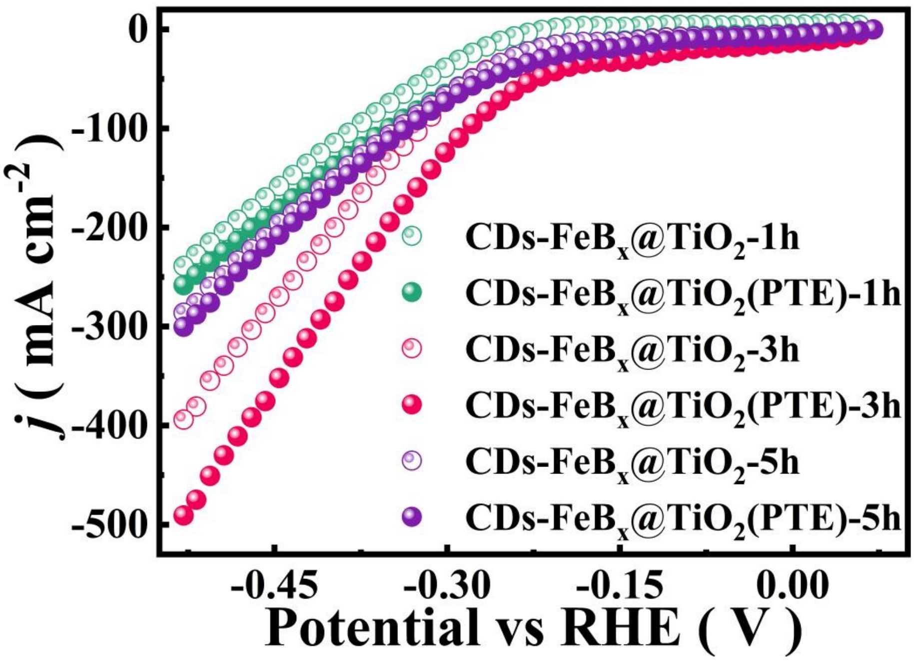

Figure S2. LSV curves of CDs-FeB_x@TiO_2 electrode with different electroless plating (EP) time during HER process.

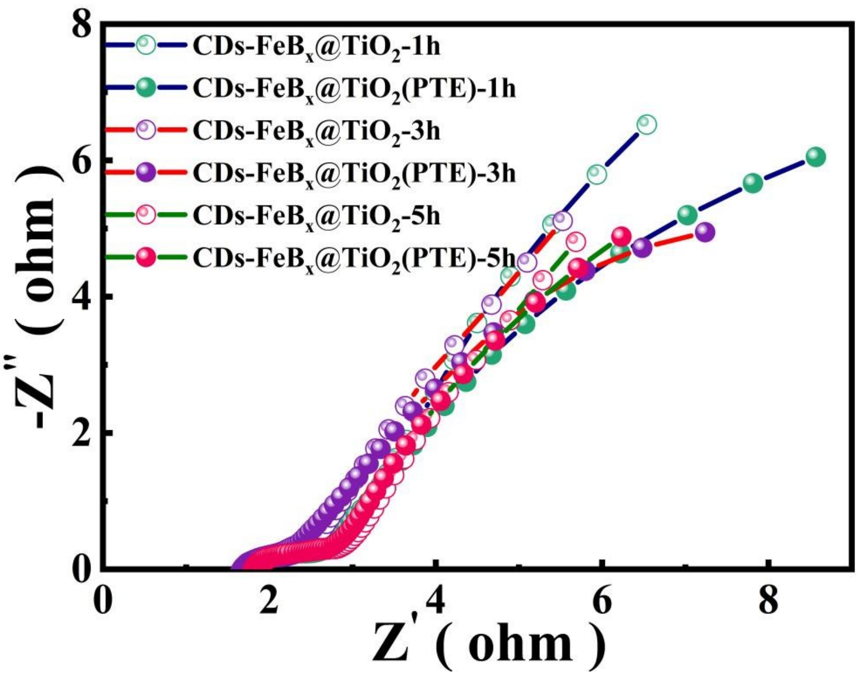

Figure S3. EIS measurements of CDs-FeB_x@TiO_2 with different EP time during HER process.

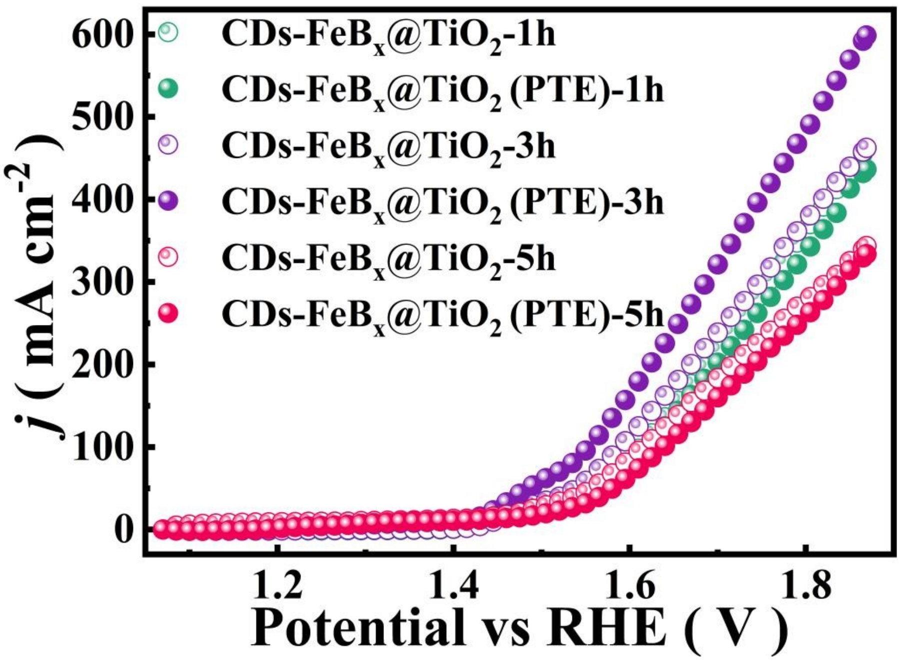

Figure S4. LSV curves of CDs-FeB_x@TiO_2 electrode with different EP time during OER process.

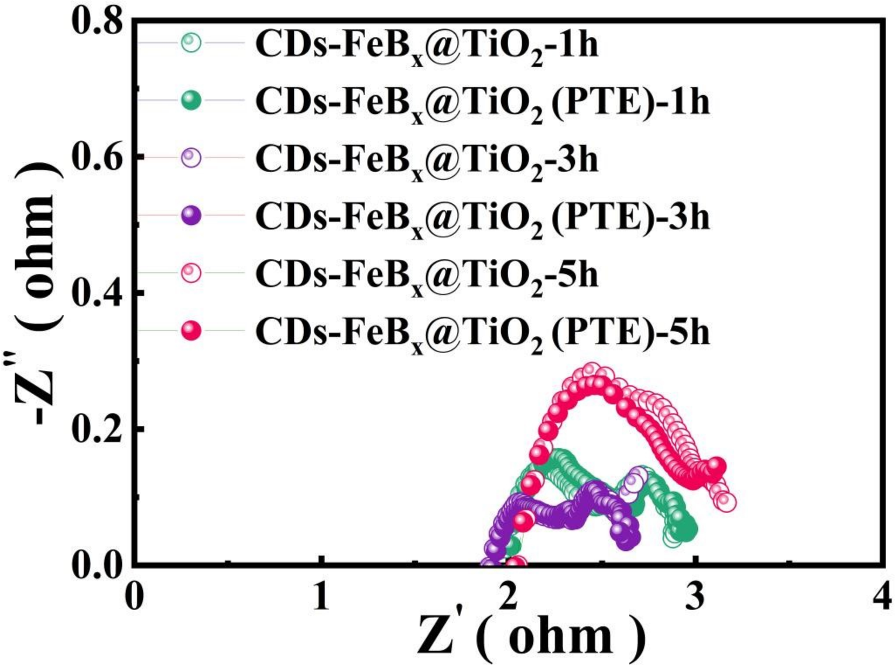

Figure S5. EIS measurements of CDs-FeB_x@TiO_2 with different EP time during OER process.

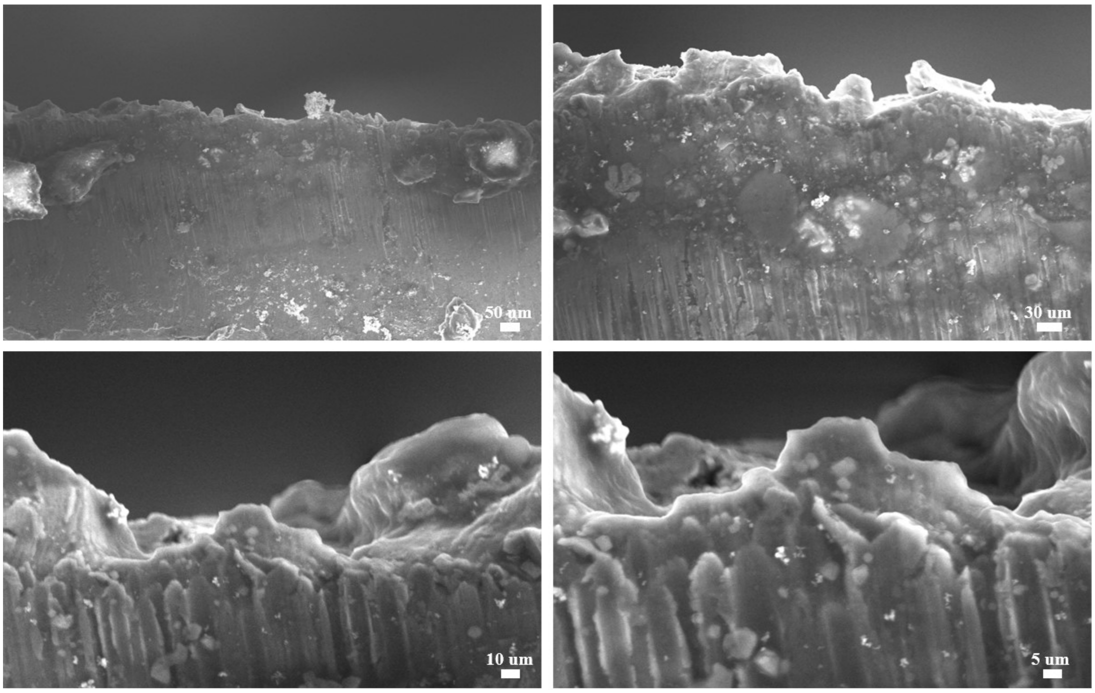

Figure S6. Cross-section SEM of CDs-FeB_x@TiO_2 at 50 um, 30 um, 10 um, 5 um, respectively.

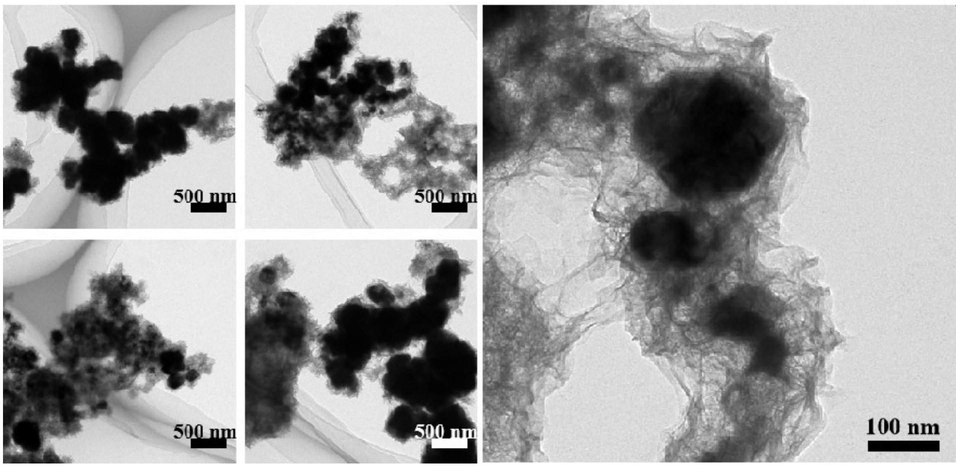

Figure S7. CDs-FeB_x@TiO_2 transmission electron microscopy at 500 nm, 100 nm, respectively.

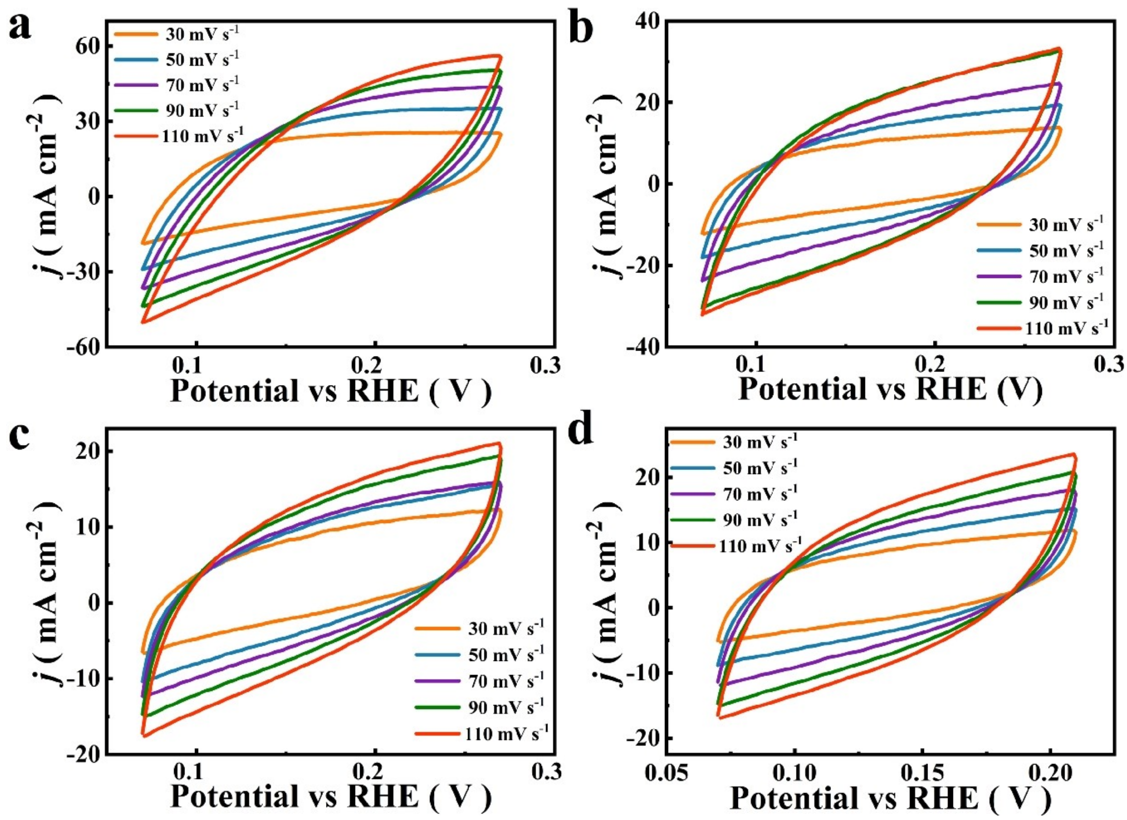

Figure S8. CV curves within a non-faradaic reaction region of 0.05~0.40 V (vs. RHE) at different scan rates toward HER for (a) CDs-FeB_x@TiO_2 PTE; (b) CDs-FeB_x@TiO_2; (c) FeB_x@TiO_2 PTE (d) FeB_x@TiO_2.

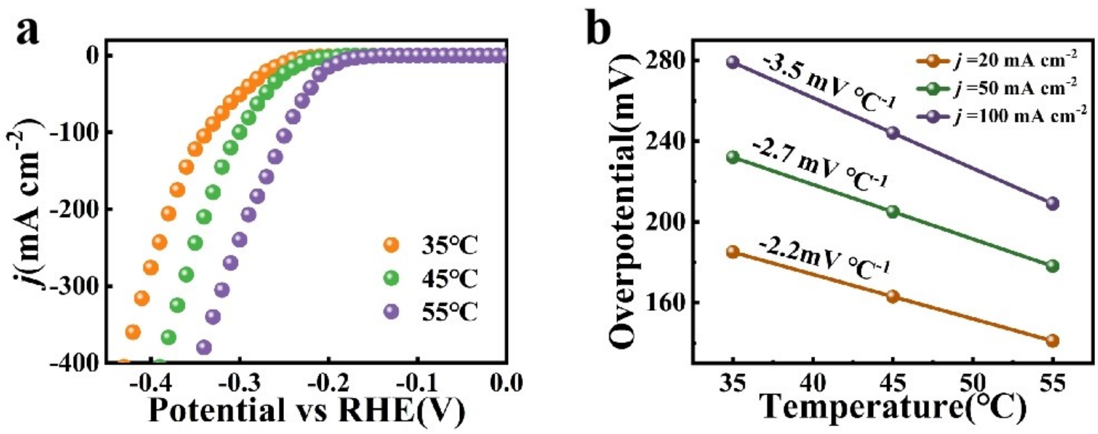

Figure S9. (a) Temperature-dependent LSV curves of CDs-FeB_x@TiO_2 PEE in 1M KOH + 0.5M NaCl by heating the temperature of electrolyte during HER process; (b) fitted curves of the relationships between overpotential and temperature at j=20, 50, 100 mA cm^{-2}, respectively.

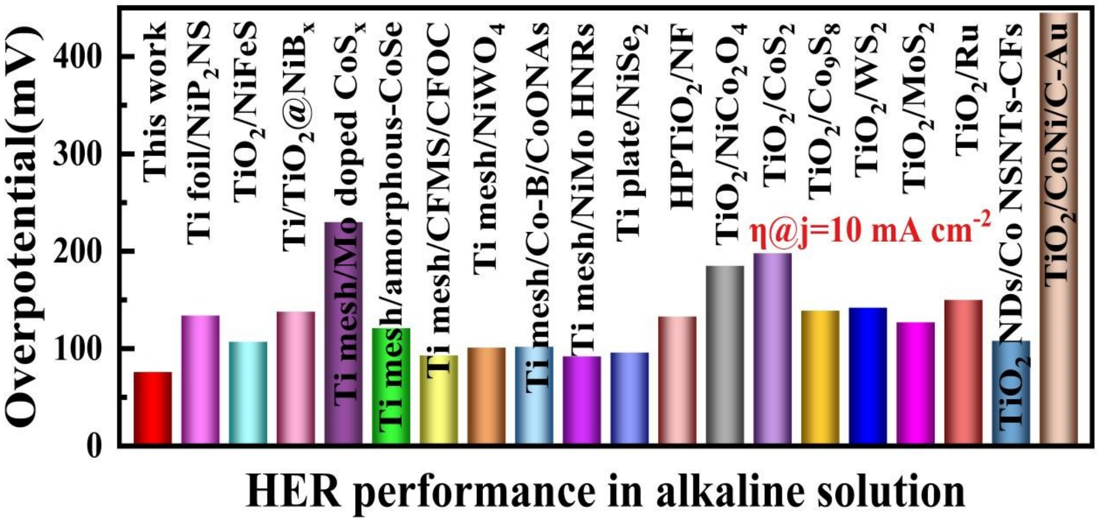

Figure S10. The HER performance of CDs-FeB_x@TiO_2 and state-of-the-art transition metal-based bifunctional electrocatalysts was compared.

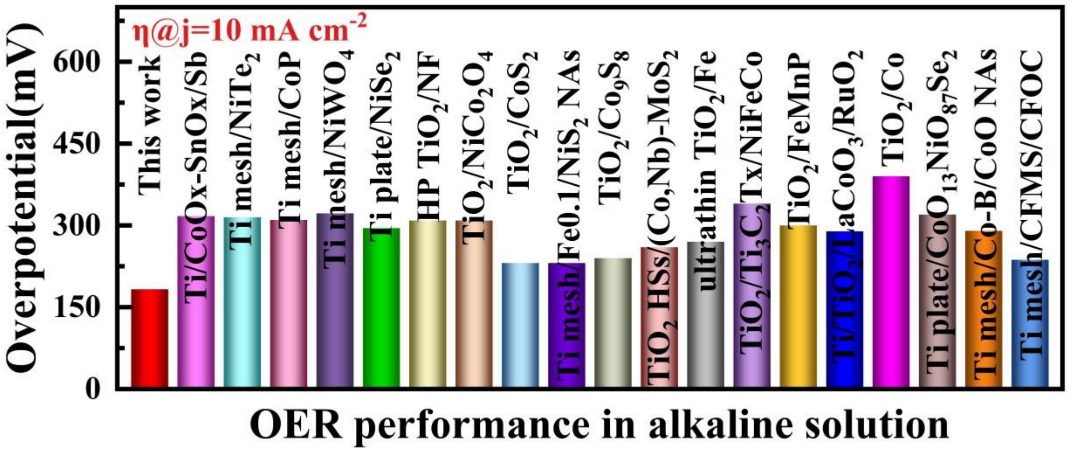

Figure S11. The OER performance of CDs-FeB_x@TiO_2 and state-of-the-art transition metal-based bifunctional electrocatalysts was compared.

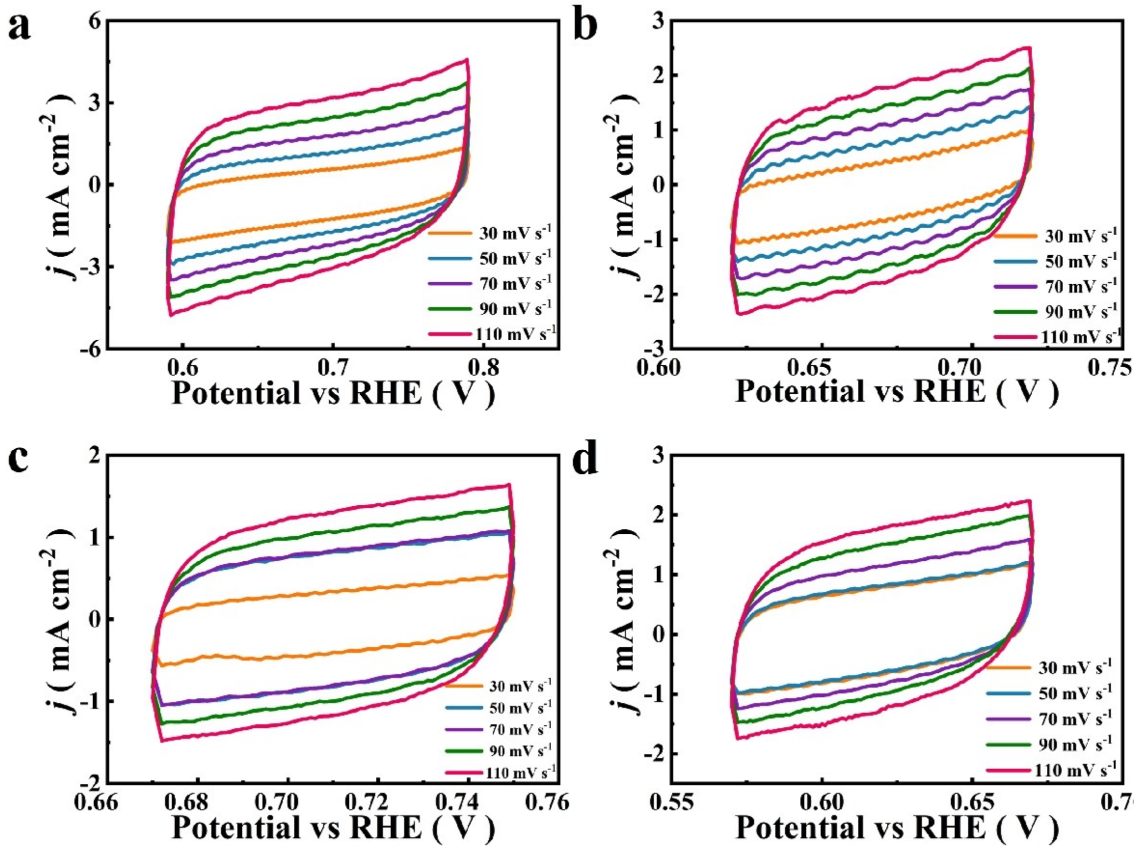

Figure S12. CV curves within a non-faradaic reaction region of 0.05~0.40 V (vs. RHE) at different scan rates toward OER for (a) CDs-FeB_x@TiO_2 PTE; (b) CDs-FeB_x@TiO_2; (c) FeB_x@TiO_2 PTE (d) FeB_x@TiO_2.

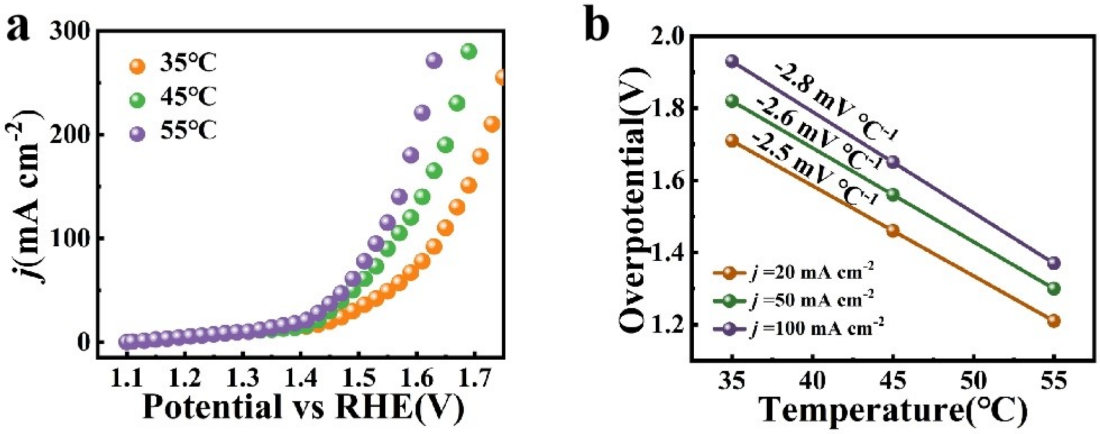

Figure S13. (a) Temperature-dependent LSV curves of CDs-FeB_x@TiO_2 PEE in 1M KOH + 0.5M NaCl by heating the temperature of electrolyte during OER process; (b) fitted curves of the relationships between overpotential and temperature at j=20, 50, 100 mA cm^{-2}, respectively.

Supporting Tables

Table S1. Comparison of HER overpotential of electrodes in 1.0 M KOH+0.5 M NaCl.

Electrode material	η10(mV)	η50(mV)	η100(mV)
CDs-FeB_x@TiO_2 1h	250	398	381
CDs-FeB_x@TiO_2 1h (PTE）	135	277	351
CDs-FeB_x@TiO_2 3h	76	245	324
CDs-FeB_x@TiO_2 3h (PTE）	56	223	282
CDs-FeB_x@TiO_2 5h	128	278	343
CDs-FeB_x@TiO_2 5h (PTE）	93	266	336

Table S2. Comparison of OER overpotential of electrodes in 1.0 M KOH+0.5 M

NaCl.

Electrode material	**η10(mV)**	**η50(mV)**	**η100(mV)**
CDs-FeB_x@TiO_2 1h	236	337	382
CDs-FeB_x@TiO_2 1h (PTE)	224	330	377
CDs-FeB_x@TiO_2 3h	187	309	359
CDs-FeB_x@TiO_2 3h (PTE)	183	254	324
CDs-FeB_x@TiO_2 5h	207	237	304
CDs-FeB_x@TiO_2 5h (PTE)	199	221	282

Table S3. HER overpotential of electrodes in 1.0 M KOH+0.5 M NaCl.

Electrode material	η10(mV)	η50(mV)	η100(mV)
Pt/C@TiO_2	397	0	0
TiO_2 (PTE)	374	0	0
FeB_x@TiO_2 3h	103	225	342
FeB_x@TiO_2 3h (PTE）	93	203	325
CDs-FeB_x@TiO_2 3h	76	179	313
CDs-FeB_x@TiO_2 3h (PTE）	56	156	286

Table S4. OER overpotential of electrodes in 1.0 M KOH+0.5 M NaCl.

Electrode material	η10(mV)	η50(mV)	η100(mV)

Pt/C@TiO_2	0	0	0
TiO_2 (PTE)	614	0	0
FeB_x@TiO_2 3h	249	298	395
FeB_x@TiO_2 3h (PTE）	216	273	357
CDs-FeB_x@TiO_2 3h	187	223	337
CDs-FeB_x@TiO_2 3h (PTE）	183	215	316

Table S5. Comparison of HER performance of CDs-FeB_x@TiO_2 electrode with recently reported titanium series catalysts in 1.0 M KOH+0.5 M NaCl.

Catalysts	Electrode	η10(mV)	Reference
CDs-FeB_x@TiO_2	1M KOH + 0.5M NaCl	56	This work
Ti foil/NiP_2NS	1M KOH	134	S1
TiO_2/NiFeS	1M KOH	107	S2
Ti/TiO_2@NiBx	1M KOH	138	S3
Ti mesh/Mo doped CoSx	1M KOH	230	S4
Ti mesh/amorphous-CoSe	1M KOH	121	S5
Ti mesh/CFMS/CFOC	1M KOH	93	S6
Ti mesh/$NiWO_4$	1M KOH	101	S7
Ti mesh/Co-B/CoONAs	1M KOH	102	S8
Ti mesh/NiMo HNRs	1M KOH	92	S9
Ti plate/$NiSe_2$	1M KOH	96	S10
HPTiO_2/NF	1M KOH	133	S11
TiO_2/$NiCo_2O_4$	1M KOH	185	S12
TiO_2/CoS_2	1M KOH	198	S13
TiO_2/Co_9S_8	1M KOH	139	S14
TiO_2/WS_2	1M KOH	142	S15
TiO_2/MoS_2	1M KOH	127	S16
TiO_2/Ru	1M KOH	150	S17
TiO_2NDs/Co NSNTs-CFs	1M KOH	108	S18
TiO_2/CoNi/C-Au	1M KOH	445	S19

Table S6. Comparison of OER performance of CDs-FeB_x@TiO_2 electrode with recently reported titanium series catalysts of electrodes in 1.0 M KOH+0.5 M NaCl.

Catalysts	Electrode	η10(mV)	Reference
CDs-FeB_x@TiO_2	1M KOH + 0.5M NaCl	183	This work

Ti/CoO_x-SnO_x/Sb	1M KOH	317	S20
Ti mesh/$NiTe_2$	1M KOH	315	S21
Ti mesh/CoP	1M KOH	310	S22
Ti mesh/$NiWO_4$	1M KOH	322	S7
Ti plate/$NiSe_2$	1M KOH	295	S10
HP TiO_2/NF	1M KOH	309	S11
TiO_2/$NiCo_2O_4$	1M KOH	309	S12
TiO_2/CoS_2	1M KOH	231	S13
Ti mesh/Fe0.1/NiS_2 NAs	1M KOH	230	S23
TiO_2/Co_9S_8	1M KOH	240	S14
TiO_2 HS_8/(Co,Nb)-MoS_2	1M KOH	260	S24
ultrathin TiO_2/Fe	1M KOH	270	S25
TiO_2/Ti_3C_2Tx/NiFeCo-LDH	1M KOH	340	S26
TiO_2/FeMnP	1M KOH	300	S27
Ti/TiO_2/$LaCoO_3$/RuO_2	1M KOH	289	S28
TiO_2/Co	1M KOH	390	S29
Ti plate/$CoO_{13}NiO_{87}Se_2$	1M KOH	320	S30
Ti mesh/Co-B/CoO NAs	1M KOH	290	S8
Ti mesh/CFMS/CFOC	1M KOH	237	S6

Table S7. Comparison of OWS performance of CDs-FeB_x@TiO_2 electrode with recently reported bifunctional catalysts in 1.0 M KOH+0.5 M NaCl.

Catalysts	**Electrode**	**Potential(V)** (*j*=10mA cm^{-2})	**Reference**
CDs-FeB_x@TiO_2	1M KOH + 0.5M NaCl	1.42	This work
NF-Ni_3S_2 /MnO_2	1M KOH	1.52	S31
NF-C/CoS/NiOOH	1M KOH	1.71	S32

CoFe/NF	1M KOH	1.64	S33
CoFeZr oxides/NF	1M KOH	1.63	S34
HOF-$Co_{0.5}Fe_{0.5}$/NF	1M KOH	1.63	S35
Fe-Ni_2P@PC/Cu_xS	1M KOH	1.62	S36
NF/T(Ni_3S_2 /MnS-O)	1M KOH	1.54	S37
FeB_2 /NF	1M KOH	1.57	S38
$NiFeO_x$@NiCu	1M KOH	1.67	S39
$CuFe_2O_4$	1M KOH	1.62	S40
Co-Cu-W	1M KOH	1.8	S41
Co@N-CNT/NF	1M KOH	1.58	S42
LIA-Ni-BDC	1M KOH	1.6	S43
NCMC/NCMC	1M KOH	1.63	S44
NiFe-MS/MOF@NF	1M KOH	1.74	S45
Co-Mo-P@NCNS	1M KOH	1.58	S46
NiFe-P@GNS	1M KOH	1.58	S47
PtCo@NC//RuCo@NC	1M KOH	1.52	S48
CoP@FeCoP/NC USMPPs	1M KOH	1.68	S49

Reference.

[1] Q.H. Cao, C.Q. Wang, S.J. Chen, X.D. Xu, F.G. Liu, X.H. Geng, J.H. Wang, Int J Hydrogen Energ, 44 (2019) 6535-6543.
[2] Y.D. Xue, Z.S. Fishman, Y.T. Wang, Z.H. Pan, X. Shen, R. Yanagi, G.S. Hutchings, M.Z. Liu, S.L. Zheng, Y. Zhang, E.I. Altman, S. Hu, J Mater Chem A, 7 (2019) 3227-3233.
[3] Y. Fu, S. Weng, J.L. Fan, Y.R. Zhang, Y.H. Guo, W.J. Hao, Chem Eng J 2022, 430, 132881.
[4] J.K. Wang, Y.J. Wang, Z.P. Yao, T.P. Xie, S.L. Liu, Z.H. Jiang, J Electrochem Soc, 167 (2020) 114510.
[5] T.T. Liu, Q. Liu, A.M. Asiri, Y.L. Luo, X.P. Sun, Chem Commun, 51 (2015) 16683-16686.
[6] J.X. Zhao, X. Ren, X. Su, Y. Zhang, T. Yan, Q. Wei, D. Wu, Chemelectrochem, 7 (2020) 2309-2313.
[7] Y.Y. Ji, L. Yang, X. Ren, G.W. Cui, X.L. Xiong, X.P. Sun, ACS Sustain Chem

Eng, 6 (2018) 9555-9559.
[8] W.B. Lu, T.T. Liu, L.S. Xie, C. Tang, D.N. Liu, S. Hao, F.L. Qu, G. Du, Y.J. Ma, A.M. Asiri, X.P. Sun, Small, 13 (2017) 1700805.
[9] J.Q. Tian, N.Y. Cheng, Q. Liu, X.P. Sun, Y.Q. He, A.M. Asiri, J Mater Chem A, 3 (2015) 20056-20059.
[10] Z.H. Pu, Y.L. Luo, A.M. Asiri, X.P. Sun, ACS Appl Mater Inter, 8 (2016) 4718-4723.
[11] Y. Yan, X. Cheng, W.W. Zhang, G. Chen, H.Y. Li, A. Konkin, Z.C. Sun, S.R. Sun, D. Wang, P. Schaaf, ACS Sustain Chem Eng, 7(2019) 885-894.
[12] R. Vadakkekara , R. Illathvalappil , S. Kurungot, Chemelectrochem, 5 (2018) 4000-4007.
[13] P. Ganesan, A. Sivanantham, S. Shanmugam, J Mater Chem A, 6 (2018) 1075-1085.
[14] S.J. Deng, Y. Zhong, Y.X. Zeng, Y.D. Wang, X.L. Wang, X.H. Lu, X.H. Xia, J.P. Tu, Adv Sci, 5 (2018) 1700772.
[15] S.H. Liu, Y.X. Xu, D. Chanda, L. Tan, R.M. Xing, X.Y. Li, L.Q. Mao, N. Kazuya, A. Fujishima, Int J Hydrogen Energ, 45 (2020) 1697-1705.
[16] L. Wang, Y.T. Qian, J.M. Du, L.Y. Zhang, G. Li, B. Zhang, W.M. Wang, D.J. Kang, J Alloy Compd, 821 (2020) 153203.
[17] S.Y. Nong, W.J. Dong, J.W. Yin, B.W. Dong, Y. Lu, X.T. Yuan, X. Wang, K.J. Bu, M.Y. Chen, S.D. Jiang, L.M. Liu, M.L. Sui, F.Q. Huang, J Am Chem Soc, 140 (2018) 5719-5727.
[18] J.X. Feng, H. Xu, Y.T. Dong, X.F. Lu, Y.X. Tong, G.R. Li, Angew Chem Int Edit, 56 (2017) 2960-2964.
[19] M.M. Wang, C. Xu, C.P. Li, Y.D. Jin, J Mater Chem A, 7 (2019) 19704-19708.
[20] M.Z. Wu, Y. Li, J. Du, C.Y. Tao, Z.H. Liu, Appl Surf Sci, 495 (2019) 143596.
[21] Z.C. Wang, L.X. Zhang, Chemelectrochem, 5 (2018) 1153-1158.
[22] L.B. Yang, H.L. Qi, C.X. Zhang, X.P. Sun, 27 (2016) 23lt01.
[23] N. Yang, C. Tang, K.Y. Wang, G. Du, A.M. Asiri, X.P. Sun, Nano Research, 9 (2016) 3346-3354.
[24] D.C. Nguyen, T.L.L. Doan, S. Prabhakaran, D.T. Tran, D. Kim, J.H. Lee, N.H. Kim, Nano Energy, 82 (2021) 105750.
[25] G.Q. Shen, R.R. Zhang, L. Pan, F. Hou, Y.J. Zhao, Z.Y. Shen, W.B. Mi, C.X. Shi, Q.F. Wang, X.W. Zhang, J.J. Zou, Angew Chem Int Edit, 59 (2020) 2313-2317.
[26] N.X. Hao, Y. Wei, J.L. Wang, Z.W. Wang, Z.H. Zhu, S.L. Zhao, M. Han, X. Huang, RSC Adv, 8 (2018) 20576-20584.
[27] D.E. Schiper, Z.H. Zhao, A.P. Leitner, L.X. Xie, F. Qin, M.K. Alam, S. Chen, D.Z. Wang, Z.F. Ren, Z.M. Wang, J.M. Bao, K.H. Whitmire, ACS Nano, 11 (2017) 4051-4059.
[28] S. Li, Y.L. Li, Z.G. Zhang, X.Y. Chen, H. Xiao, L. Lin, W.Q. Wu, X.Y. Wu, X.Y. Jiang, J Appl Electrochem, 50 (2020) 723-731.
[29] Y. Yan, C.Y. Liu, H.W. Jian, X. Cheng, T. Hu, D. Wang, L. Shang, G. Chen, P. Schaaf, X.Y. Wang, E. Kan, T.R. Zhang, Adv Funct Mater, 31 (2021) 2009610.
[30] T.T. Liu, A.M. Asiri, X.P. Sun, Nanoscale, 8 (2016) 3911-3915.

[31] Y. Xiong, L. Xu, C. Jin, Q. Sun, Appl. Catal., B 2019, 254, 329.
[32] F. T. Tsai, Y. T. Deng, C. W. Pao, J. L. Chen, J. F. Lee, K. T. Lai, W. F. Liaw, J. Mater. Chem. A 2020, 8, 9939.
[33] P. Babar, A. Lokhande, H. H. Shin, B. Pawar, M. G. Gang, S. Pawar, J. H. Kim, Small 2018, 14, 1702568.
[34] L. Huang, D. Chen, G. Luo, Y. R. Lu, C. Chen, Y. Zou, C. L. Dong, Y. Li, S. Wang, 40 Adv. Mater. 2019, 31, 1901439.
[35] F. Q. Liu, J. W. Liu, Z. Gao, L. Wang, X. Z. Fu, L. X. Yang, Y. Tao, W. H. Yin, F. Luo, Appl. Catal., B 2019, 258, 117973.
[36] D. T. Tran, H. T. Le, V. H. Hoa, N. H. Kim and J. H. Lee, Nano Energy, 2021, 84, 105861.
[37] Y. Zhang, J. Fu, H. Zhao, R. Jiang, F. Tian, R. Zhang, Appl. Catal., B 2019, 257, 117899.
[38] H. Li, P. Wen, Q. Li, C. Dun, J. Xing, C. Lu, S. Adhikari, L. Jiang, D. L. Carroll, S. M. Geyer, Adv. Energy Mater. 2017, 7, 1700513.
[39] Y. Zhou, Z. Wang, Z. Pan, L. Liu, J. Xi, X. Luo and Y. Shen, Adv Mater, 2019, 31, 1806769.
[40] V. Sharma, U. N. Pan, T. I. Singh, A. K. Das, N. H. Kim and J. H. Lee, Chem 33 Eng J, 2021, 415, 127779.
[41] D. Gao, R. Liu, J. Biskupek, U. Kaiser, Y. Song and C. Streb, Angew Chem Int Edit, 2019, 58, 4644-4648.
[42] L. Yang, H. Li, Y. Yu, Y. Wu, L. Zhang, Appl Catal B-Environ 2020, 271, 118939.
[43] Y. J. Tang, H. Zheng, Y. Wang, W. Zhang, K. Zhou, Adv Funct Mater 2021, 31, 2102648.
[44] X. Wei, Y. Zhang, H. He, D. Gao, J. Hu, H. Peng, L. Peng, S. Xiao, P. Xiao, Chem Commun 2019, 55, 6515-6518.
[45] M. Zhao, W. Li, J. Li, W. Hu, C. M. Li, Adv Sci 2020, 7, 2001965.
[46] N. Li, Y. Guan, Y. Li, H. Mi, L. Deng, L. Sun, Q. Zhang, C. He, X. Ren, J Mater Chem A 2021, 9, 1143-1149.
[47] D. Yang, Z. Su, Y. Chen, Y. Lu, B. Yu, K. Srinivas, B. Wang, W. Zhang, J Mater Chem A 2020, 8, 22222-22229.
[48] B. Sarkar, D. Das, K. K. Nanda, Green Chem 2020, 22, 7884-7895.
[49] J. Shi, F. Qiu, W. Yuan, M. Guo, Z.-H. Lu, Chem Eng J 2021, 403, 126312.